Small-Amplitude Atomic Force Microscopy

Peter M. Hoffmann
Department of Physics, Wayne State University, Detroit, MI 48201, USA

March 10, 2004

Introduction

Small amplitude Atomic Force Microscopy (AFM) is a dynamic AFM technique, in which the AFM cantilever is vibrated at very small amplitudes, typically less than ≈ 1 Å $(= 10^{-10}$ m $=$ 0.1 nm), and the amplitude, phase and/ or resonance frequency of the lever are measured. Small amplitudes serve to *linearize* measurements of tip-surface interactions. Consequently, measurements can be directly related to interaction stiffness (negative if the force gradient) and energy dissipation. Because of the small amplitudes, the measurement is *local*, and interactions can be mapped point-by-point. This eliminates ambiguities present in large amplitude techniques.

Historically, Scanning Tunneling Microscopy (STM) [1] was the first 'easy' technique to reliably provide atomic resolution images of a variety of *conductive* crystalline surfaces. Early on it was realized that forces play an important role in Scanning Tunneling Microscopy (STM) measurements [2]. This inspired the invention of the Atomic Force Microscope (AFM) in 1986 [3]. In terms of applications, it was hoped that AFM would provide atomic resolution on insulators, which was not possible with STM. This goal was finally achieved in 1995, when true atomic resolution imaging was demonstrated by several groups using dynamic, non-contact AFM at *large* amplitudes [4–6]. Researchers also realized early on that AFM can be used to measure forces as a function of tip-surface separation in a variety of environments [7–10]. However, issues like drift, mechanical instabilities [11], low sensitivity, and non-linearities made the direct, local and linear measurement of force interactions a difficult prospect in many situations.

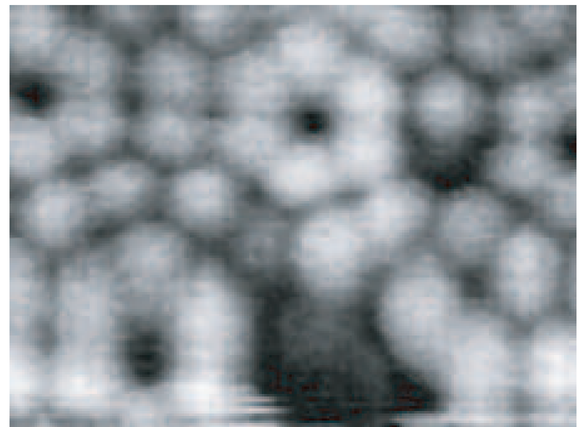

Figure 1: Atomic resolution image (4 x 2.5 nm) of the force gradient across a Si(111)-(7x7) surface. Round 'bumps' correspond to single atoms. Measured with a sub-resonance AFM at an ultra-small lever amplitude of 0.25 Å. Feedback was maintained via the tunneling current.

Small amplitude AFM techniques were developed to address the issues of non-linearity and non-locality that continue to plague large amplitude measurements. Moreover, combined with high sensitivity deflection sensors, such as fiber interferometry, and the use of tailored lever structures, these techniques were able to overcome sensitivity and instability issues as well. In this chapter we will discuss the underlying theory of small amplitude AFM, conditions and limitations for its use, and recent examples of small amplitude AFM applied to atomic scale imaging, force-distance measurements, atomic scale dissipation, and force measurements in liquids.

Theory and Background

Limitations of 'standard' AFM techniques

Commonly used AFM technologies can be categorized into two broad categories: (1) 'DC' or 'contact' AFM and (2) 'AC' or 'dynamic' AFM. Here, 'dc' is meant to signify a static technique, while "ac" is meant to signify a dynamic technique, involving modulation of the deflection or force. In DC AFM the cantilever is static and the equilibrium position of the cantilever in the force field of the sample is measured. The force can then be determined from Hooke's law. In AC AFM the cantilever is vibrated and typically two of the observables amplitude, phase, or resonance frequency are measured to determine the tip-sample interaction.

In the following we want to discuss limitations of DC and *large amplitude* AC techniques, which range from drift, mechanical instabilities, nonlinearity to problems of data interpretation.

Limitations of DC and large amplitude AC AFM techniques

DC AFM suffers like any DC measuring technique from low signal-to-noise and drift. Therefore, DC AFM generally utilizes low stiffness levers in order to increase sensitivity ($< 1\text{Nm}^{-1}$). Because of the low stiffness of the lever, it is prone to the snap-to-contact instability close to surface [11–13]. Consequently, DC AFM is generally known as 'contact' AFM. This type of AFM is useful in general purpose imaging at resolutions typically > 10 nm. It is theoretically able to directly yield quantitative force data (via Hooke's law). However, this is generally hampered by drift and the snap-in instability.

DC AFM also has limitations in imaging. Since imaging is generally done in contact, the image resolution is limited to the tip-surface contact radius, which is typically at least several tens of nanometers. In some special cases true atomic resolution has been achieved [14], but typically, apparent 'atomic resolution' seen with contact AFM can be attributed to a Moiré-like effect of dragging two well-ordered surfaces (tip and substrate) across each other [15, 16]. Another disadvantage is the fact that the tip is moved laterally while in contact and that sometimes relatively large forces need to be applied to get a reasonable signal. This can lead to wear and degradation of the sample and tip [17], and is especially detrimental to soft samples.

In order to overcome some of the disadvantages of DC AFM, AC AFM techniques were employed almost as soon as the AFM was invented [8]. There are two major types of AC AFM techniques [18]: (1) Amplitude modulated (AM) AFM, which includes tapping mode AFM, some types of non-contact AFM and sub-resonance AFM, and (2) Frequency modulated (FM) AFM,

or frequency-shift AFM, also often confusingly called non-contact AFM.

In AM AFM the lever is vibrated at a *constant* frequency, and the amplitude and/or phase are measured. This is typically done with a lock-in amplifier. In 'tapping mode' AFM [19], the cantilever is brought close to the surface while it is vibrated at (or close to) the free resonance frequency of the lever. As the tip approaches the surface, the resonance frequency shifts due to the interaction force gradients. Since the lever is still vibrated at the free resonance frequency, both the phase and the amplitude of the cantilever decrease and can be used as feedback parameters (slope detection).

Tapping mode AFM typically uses large amplitudes of 10-100 nm. As the tip moves through the non-linear force field close to the surface, the motion of the lever becomes highly non-linear. Typically the system is bistable, and jumps between a low amplitude and high amplitude mode are inherent to the system [18, 20–23]. In addition, relatively low stiffness cantilevers are typically used (of the order of a few 10 N/m) to boost sensitivity. As a result, the tip is unstable close to the surface and starts 'tapping' the surface, hence the name of the technique. This could be avoided by using stiffer cantilevers [24], but that would reduce the signal unduly. Due to the intermittent contact with the surface, the resolution of this technique is comparable to contact AFM. However, since the tip is not dragged across the surface as in contact AFM, the damage to a fragile sample can be much less than in contact AFM [19]. In addition, the phase data contains information about sample mediated damping and can provide additional information about the mechanical properties of the sample. However, while attempts have been made to interpret the results in a quantitative fashion, it is very difficult to completely reconstruct the force field and the distance-dependent loss processes experienced by the tip, and higher resonance modes need to be taken into account [25, 26].

Non-contact AM AFM [8] is essentially the same as tapping mode AFM, with the only difference being that the tip is lifted off the surface far enough to avoid contact. Non-contact AM AFM is typically used to measure long-range forces such as electrostatic forces (Electrostatic Force Microscopy: EFM) or magnetic forces (Magnetic Force Microscopy: MFM).

In FM AFM the lever is vibrated at its (shifting) resonance at all times. Typically (but not always) a feedback loop is used to keep the amplitude constant. The lever is maintained at its resonance frequency by using the lever itself as the frequency determining element in an oscillator circuit. This is achieved by phase shifting the deflection signal and feeding it back to the dither piezo that oscillates the cantilever. The resonance frequency is then measured by an FM demodulator circuit [27]. The resonance frequency can be measured very accurately for high quality factor (Q) cantilevers, providing improved signal-to-noise (S/N) ratios. Because a high Q ($\approx 10^3 - 10^4$) is needed, FM AFM is most often used in ultra-high vacuum (UHV). The improved S/N ratio allows for the use of higher stiffness levers of typically about 50 Nm^{-1}. The use of stiffer levers combined with large amplitudes [28, 29] avoids the snap-to-contact instability and non-contact operation very close to the surface becomes possible. Indeed it was this technique that yielded the first true atomic resolution AFM images in 1994 [4] and 1995 [5, 6]. The problems with this technique are the very involved data interpretation when using large amplitudes [25, 30, 31], the difficulties in measuring local events (because of the large am-

plitudes), and the almost complete confinement of this technique to ultra-high vacuum conditions (because of the need for high Q). Recently, using an electronic feedback circuit, attempts have been made to increase the low quality factor ($Q \approx 2-3$) of nc-AFM in water to $Q \approx 30-40$ [32]. However, these low Q values are still too low to achieve atomic resolution in liquids, and the used techniques raise additional interpretation issues.

Theory of small amplitude AFM

Small amplitude AFM is any dynamic AFM technique, in which particular attention is paid to vibrating the cantilever at small amplitudes. This means in practice that amplitudes should be small compared to the range of the measured interaction. How small the amplitude has to be in order to justifiably speak of *linear* measurements can be explored by solving the equation of motion of the oscillating cantilever in the force field of the sample. In addition, by solving the equation of motion, we can distinguish between several conceivable ways of operating a small amplitude AFM. These include:

1. On-resonance AM operation ('tapping mode'): AM AFM where we drive the cantilever at small amplitudes at a constant frequency close to or at the free resonance frequency. Amplitude and phase are measured and can, in principle, be related directly to the force gradient and damping coefficient.

2. Sub-resonance operation: AFM is deliberately operated at a constant frequency well below the first resonance. This eliminates dynamic terms in the equation of motion, and makes it easier to keep the AFM in the small amplitude regime. Measured amplitude and phase relate directly to the force gradient and damping.

3. Frequency shift (FM) operation: Same as regular FM AFM, but using ultra-small amplitudes. In this case, the frequency shift can be directly related to the force gradient (see below). The cantilever amplitude (or the excitation amplitude if amplitude is kept constant) can be related to the damping coefficient or quality factor.

4. Force controlled or force modulation AFM: AFM in which a force rather than a displacement is imposed on the cantilever. Typically a DC and AC force are applied, and force and stiffness are measured simultaneously. Often used in the sub-resonance regime.

Actual examples of these different techniques will be discussed towards the end of the chapter.

Small amplitude AFM

The general equation of motion of AFM is given by:

$$m^* \ddot{z} + C\dot{z} + k_L z = k_L A_0 \exp(i\omega t) + F_{ts}(z+d) \quad (1)$$

Here, m^* is the effective vibrating mass of cantilever & tip, z is the cantilever deflection, d is the average tip-surface separation, C is the damping coefficient, k_L is the lever stiffness, and A_0 is the applied amplitude (which is equal to the free amplitude in the off-resonance case). If the AFM is operated in the force modulated mode, the equation is modified by replacing $k_L A_0$ on the right-hand side by F_0, the modulated force.

F_{ts} is the sum of forces acting between the tip and the surface. F_{ts} generally consists of several forces with different interaction ranges. In vacuum, the forces present include chemical bonding, Van-der-Waals forces, electrostatic forces or magnetic forces. In liquids, we also encounter forces associated with the medium such as solvation forces and hydrophilic/hydrophobic interactions [33]. In ambient, capillary forces can be very important. When writing expressions for F_{ts}, we also need to be careful that forces act on different portions of the tip depending on their range. Long-range forces, like electrostatic forces in the presence of an applied voltage, might act on the entire vibrating cantilever, while short-range forces, such as chemical bonding forces act on the outermost atoms of the tip only. Finally, we have to take into account that the tip and surface are not infinitely rigid, but instead deform under the influence of the force field. This leads to a re-scaling of the tip-surface separation z [13, 34]. However, to simplify the discussion, we will ignore these effects for the time being.

In equation (1) the cantilever is being treated as a linear spring which is a very good approximation for the small amplitudes involved [35]. We also assumed that the damping coefficient, C, is independent of tip position. This is in general not true, but again is a good local approximation if small amplitudes are used.

Generally, because of the non-linear nature of the force field, F_{sr}, equation (1) can only be solved numerically. In some special cases, analytic solutions can be found. A very special case occurs when the AFM is operated at amplitudes over which the force law can be approximately considered linear. We can then write $F_{ts} = F_{ts,0} - k_{ts}z$. For convenience, we re-scale the displacement z to account for the equilibrium position of the cantilever $z_0 = F_{ts,0}/k_L$, according to $z - z_0 \to z$. By doing this, z becomes a measure for the *deviation* from the equilibrium position due to the imposed oscillation. The new *linearized* equation of motion becomes:

$$m^*\ddot{z} + C\dot{z} + (k_L + k_{ts})z = k_L A_0 \exp(i\omega t) \quad (2)$$

Note that the interaction stiffness, k_{ts}, is the negative of the force gradient, $\frac{\partial F}{\partial z}$. The steady-state solution of equation (2) is $z(t) = A\exp(i\omega t)$ where A is a complex number that includes the phase information. A is given by:

$$A = \frac{k_L A_0}{k_L + k_{ts} - \omega^2 m^* + i\omega C} \quad (3)$$

The resonance frequency in the linear regime is given by $\omega_0 = \sqrt{\frac{k_L + k_{ts}}{m^*}}$. Using this we can find for the absolute value of the amplitude:

$$|A| = \frac{k_L A_0}{\sqrt{(k_L + k_{ts})^2 (1 - \frac{\omega^2}{\omega_0^2})^2 + (C\omega)^2}} \quad (4)$$

and the phase angle between the A_0 (the drive) and A (the cantilever):

$$\tan\phi = -\frac{\omega C}{(k_L + k_{ts})(1 - \frac{\omega^2}{\omega_0^2})} \quad (5)$$

Small amplitude tapping mode AFM

In the case of tapping mode AFM, the system is driven at or near the free resonance. Since the drive frequency is kept constant, the amplitude and/or phase are measured and used as possible feedback signals. When the lever is driven at the free resonance frequency, $\omega = \omega_{0f} = \sqrt{\frac{k_L}{m^*}}$, the absolute value of the amplitude is given by (equations (4), (5)):

$$|A| = \frac{k_L A_0}{k_{ts}} \cos\phi \quad (6)$$

The phase angle is given by:

$$\tan\phi = -\frac{\omega_{0f} C}{k_{ts}} \quad (7)$$

It is straightforward to solve these equations for k_{ts} and C, and thus, at least in principle, a measurement of the amplitude and the phase are sufficient to determine the interaction stiffness and the damping.

This is to be contrasted from the usually used *large* amplitudes. In this case, the interaction and damping are very difficult to reconstruct from the amplitude and phase, since these are the result of an *integral* over the *entire* motion of the cantilever. Thus, in the case of large amplitudes we are not mapping two observables (amplitude and phase) to two unknowns (the local stiffness and damping coefficient), but instead we are trying to map our two observables to *all* values of interaction stiffness and damping coefficient the tip encounters during its trajectory. This is - without additional information - in principle impossible. Additional information might come from amplitudes and phases of higher vibration modes [25,26] or from multiple measurements at different separations and amplitudes. The interpretation , if not impossible in principle, becomes very involved.

Sub-resonance AFM

Combining equations (4) and (5), we find that the measured interactions stiffness, k_{ts}, can be determined directly from the measured amplitude and phase via:

$$k_{ts} = k_L\left(\frac{A_0 \cos\phi}{|A|(1-\frac{\omega^2}{\omega_0^2})} - 1\right) \quad (8)$$

If we keep the drive frequency, ω, well below the first resonance we can use this equation to find the following simple expression for the interaction stiffness:

$$k_{ts} = k_L\left(\frac{A_0}{|A|}\cos\phi - 1\right) \quad (9)$$

If the AFM is operated reasonably far below the resonance, the phase angle typically is very small, and the $\cos\phi$ term can in many cases be replaced by unity, resulting in:

$$k_{ts} = k_L\left(\frac{A_0}{|A|} - 1\right) \quad (10)$$

The same result can be obtained if we realize that by operating the AFM in the sub-resonance regime, the measurement becomes *quasistatic.* Close to the surface, the cantilever and interaction stiffnesses can be considered as two 'springs' in series. Thus the forces in each 'spring' are identical and we can write: $F = k_{ts}|A| = k_L(A_0 - |A|)$ which leads to the same result (10).

The damping coefficient can be calculated from:

$$C = \frac{k_L A_0}{|A|\omega} \sin\phi \quad (11)$$

Thus again a measurement of the amplitude and phase are sufficient to determine both the interaction stiffness and the damping coefficient.

Frequency shift AFM

In frequency shift AFM, the excitation frequency of the cantilever is altered to keep the lever at

its resonance at all times. Therefore the frequency becomes an observable in the measurement. At very small amplitudes [36], the resonance frequency is directly related to k_{ts}, since $\omega_0 = \sqrt{\frac{k_L + k_{ts}}{m^*}}$ (see equation (2) and reference [27]). In terms of the *free* resonance frequency, ω_{0f}, the interaction stiffness can be found from:

$$k_{ts} = k_L\left(\frac{\omega_0^2}{\omega_{0f}^2} - 1\right) \tag{12}$$

This can be approximately written in terms of the frequency shift, $\Delta f = \frac{1}{2\pi}(\omega_0 - \omega_{0f})$ as:

$$k_{ts} = 2k_L\frac{\Delta f}{f_{0f}} \tag{13}$$

The amplitude can be calculated from (4). Introducing the quality factor $Q = \frac{\omega_{0f} m^*}{C}$, we find [38]:

$$|A| = \frac{QA_0}{\sqrt{\frac{k_L + k_{ts}}{k_L}}} \approx QA_0\left(1 - \frac{k_{ts}}{2k_L}\right) \tag{14}$$

In FM AFM, the amplitude is often held constant by a feedback loop, and the excitation amplitude needed to keep a certain constant lever amplitude is measured and related to the damping [37].

In conclusion, by measuring the amplitude and the *frequency*, the interaction stiffness and the damping coefficient (or quality factor) can be determined. At larger amplitudes, the frequency shift is determined by an integral over the entire tip trajectory, and interpretation of the frequency shift data becomes much more involved [25, 28–31].

Force modulation AFM

In the case of force modulation AFM, equations (4) and (5) still hold, if we replace $k_L A_0$ by the modulated force F_0 [15]. If a small *sub-resonance* force modulation is applied to the cantilever and the displacement response is measured, these equations simplify to:

$$k_{ts} = \frac{F_0}{|A|} - k_L \tag{15}$$

which for small phase angles is simply an expression of Hooke's law, i. e. the total effective stiffness $k_{ts} + k_L$ is given by $F_0/|A|$. Note that in the case of force modulated AFM, the cantilever and interaction stiffnesses are to be considered *in parallel*, while in 'usual' displacement modulated AFM, they are to be taken to be *in series*. The reason is that in force modulated AFM, both the sample and the cantilever base are held fixed, and thus the *amplitudes* of the base-tip and tip-surface separations are identical, while the forces are different. In 'usual' AFM it is the *forces* between base & tip and tip & surface that are identical, while the amplitudes are different (A_0 versus $|A|$).

The damping coefficient in force modulated AFM can be found from:

$$C = -\frac{F_0}{|A|\omega}\sin\phi \tag{16}$$

Practical considerations

As we have seen above, the interpretation of the data becomes greatly simplified if amplitudes are small enough to consider the force field to be linear over the range of motion of the cantilever. In all four cases (tapping mode, off-resonance AM AFM, FM AFM, and force modulation AFM), both the interaction stiffness and the damping

can in principle be directly measured. In all cases, two parameters are needed: In AM and force modulated AFM we need amplitude and phase, and in FM AFM amplitude and frequency shift.

In reality, quantitative small amplitude measurements have been used quite frequently in off-resonance measurements (both displacement and force modulated), less frequently in FM AFM, and hardly at all in tapping mode experiments. The main reasons for this are problems of phase and amplitude stability in tapping mode. Since the drive frequency enters the equations, but is not explicitly measured as in FM AFM, a shift in the drive frequency can greatly affect the obtained results. Indeed a shift to higher or lower frequency than the free amplitude can lead to a bistable behavior of the oscillator if the amplitude is not small enough. Keeping the amplitude small enough, on the other hand, is difficult if the cantilever is operated near its resonance. In sub-resonance AFM, this problem is avoided by staying far below the resonance, and, as a result, the frequency does not enter into the equations and the amplitude can be kept low.

In FM AFM the lever is deliberately run at resonance, and the frequency should be quite stable if the Q of the lever is sufficiently high. The needed high Q, however, results in larger amplitudes, thus violating the small amplitude condition. If the amplitudes are deliberately kept small, thermal noise can greatly influence the measurements, since most of the thermal vibration energy is centered around the lever resonance. For a lever of 40 N/m stiffness, which is typical for FM AFM, the thermal vibration amplitude is of the order of $\sqrt{k_B T/k_L} = 0.1$Å which is of the same order as the amplitude needed to linearize measurements of atomic bonding forces. This particular problem can be alleviated by increasing the lever stiffness and sensitivity of the system as recently demonstrated by Giessibl [39].

Operating conditions of small amplitude AFM

Limits of linearity or how small is small enough ?

As shown above, the linearized equation of motion (2) can be solved in a variety of situations and leads to the simple relation (9) for the interaction stiffness in the case of an AFM operated at small amplitudes and sub-resonance frequencies, and to (13) in the case of a small amplitude, frequency shift AFM. However, an important question remains unanswered: Under what circumstances can the system be regarded linear? Or, in other words: when is the amplitude small enough ?

This question can not be answered in general, because it strongly depends on the nature of the force law that the tip encounters. Long-range forces, such as electrostatic, magnetic, and van-der-Waals forces can generally be explored with somewhat larger amplitudes. Short-range forces, such as chemical bonding and solvation forces associated with small molecules, require significantly smaller amplitudes. We might also expect that it depends on the particular AFM technique used, but, at least as a rule of thumb, the results seem to be quite similar for different AC AFM techniques.

In the case of frequency shift (FM) AFM and short-range forces, Hölscher et al. [36] showed that the frequency shift is determined by the force gradient only if the amplitudes used are in the sub-Ångstrom range, typically of the order of a few tenths of an Ångstrom. Similar results can

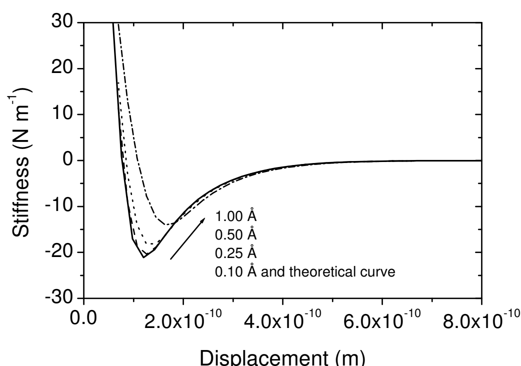

Figure 2: Simulation of the measured interaction stiffness - displacement curve for different cantilever amplitudes in a sub-resonance AM AFM. For $A_0 = 0.1$Å the measurement does not visibly deviate from the theoretical curve, at 0.25 Å there is a small error around the minimum, at 0.5 Å this error is about 10%, while at an amplitude of 1.0 Å the error has become quite large.

be obtained for sub-resonance AM AFM [34]. In a recent simulation [34] of a vibrating lever in a short-range force field (with a decay parameter of 0.54 Å), it was found that the error of the measurement was negligible for a lever amplitude of 0.1 Å, very small for an amplitude of 0.25 Å, and about 10% for an amplitude of 0.5 Å, i.e. for an amplitude of the order of the decay parameter. For large amplitudes, e.g. 1 Å, the error was quite significant. This is shown in **Figure 2**. For comparison, typical lever amplitudes in tapping mode are of the order of 100 - 1000 Å, and in FM AFM of the order of 10 - 100 Å. In the case of sub-resonance AFM, we also have the added question of the influence of the frequency, i.e. how far below the resonance we need to be to avoid resonance enhancement of the amplitude. It was found that very clean sub-resonance operation could be achieved up to about 1/8 of the resonance frequency, but acceptable error rates (< 10%) could be achieved up to frequencies of 1/3 of the free resonance. Beyond these values, the amplitude has a tendency to become too large because of resonance enhancement, complicating the interpretation of the data.

Limits of stability

Even if small drive amplitudes are used, there is no guarantee that the actual lever amplitude remains small. One reason for this is resonance enhancement, as discussed above. The other reason is the use of low stiffness cantilevers. Low stiffness cantilevers not only exhibit larger deflections in an attractive force field than higher stiffness ones, but moreover, they can become unstable and 'snap' to the surface ('snap-to-contact') [11].

In DC AFM there is a straight-forward criterion that must be satisfied if snap-to-contact is to be avoided. As long as the *effective* stiffness of the cantilever is positive, no snap-in occurs:

$$k_L + k_{ts} > 0 \tag{17}$$

This means that snap-in occurs when the interaction stiffness is negative ('attractive') and its absolute value exceeds the lever stiffness.

In AC AFM snap-in can still be avoided *even* if condition (17) is violated. The reason is that in order for snap-in to occur the total force (cantilever + interaction) must be negative (attractive) [28]. In AC AFM, the cantilever deflects beyond its equilibrium point and therefore the restoring force can overwhelm the attractive force between the tip and the surface. The second criterion for snap-in to be avoided can thus be written as:

$$k_L A + F_{ts} > 0 \tag{18}$$

This is one of the reasons for the stability of large amplitude FM AFM. In these techniques relatively low stiffness cantilevers can be used, which boost sensitivity, but because of the large amplitudes the snap-in instability can be avoided. In small amplitude methods, we need to mostly rely on criterion (17) and thus high stiffness cantilevers need to be used. This necessitates high sensitivity deflection sensing as discussed in the next subsection.

Sensitivity

Small amplitude AFM requires higher sensitivity of the deflection sensor than regular AFM. The reason is not only that small amplitudes are more difficult to measure, but also, as we have seen above, the stability criterion demands that high stiffness levers are used which reduce the signals even further. There are many ways of sensing the deflection of the cantilever [40], from tunneling as used in the original AFM [3] to the now most commonly used optical techniques. For each of these methods, a theoretical sensitivity limit can be calculated [41]. However, in reality the experimental sensitivity is typically lower due to non-ideal experimental conditions.

Since small amplitude AM AFM needs to operate preferably at amplitudes of a few tenths of an Ångstrom, the deflection sensor needs to be able to sense changes in the amplitude of the order of 0.01 Å(i.e. 1 pm) or better. This is difficult to achieve with commonly used laser deflection systems. Theoretically, highly optimized laser deflection systems might be able reach similar sensitivity than interferometer based systems [42], however, in practice, most can not sense changes in amplitude much smaller than 0.1 Å. Experimentally, it has been demonstrated that fiber interferometers [43] can have at least 10-20 times higher sensitivity than laser deflection systems and are thus the method of choice in small amplitude AM AFM.

In FM AFM, when high stiffness cantilevers are used, the frequency shift is reduced and a high sensitivity frequency measurements becomes essential. A very high Q cantilever is needed to achieve the needed sensitivity. High Q, however, leads to increased resonance enhancement of the amplitude, and thus drive amplitudes need to extremely small. Fortunately, high stiffness cantilevers also help to reduce the thermal noise at resonance, and measurements at sub-Ångstrom lever amplitudes can be achieved.

Thermal noise

When we deal with cantilever amplitudes of the order of 0.1 Å, we immediately face the question how this compares with the average amplitude of the thermal excitation of the cantilever. It can be shown [44] that the power spectral density of the oscillator amplitude due to thermal excitation is given by:

$$\langle P^2(\omega)\rangle = \frac{4k_BTC}{(k_L + k_{ts} - m\omega^2)^2 + C^2\omega^2} \tag{19}$$

Note that $\langle P^2\rangle$ has units of $\mathrm{m^2Hz^{-1}}$, i.e. it needs to be multiplied with the measurement bandwidth, B, to calculate the rms amplitude due to the thermal motion of the cantilever. The rms amplitude is given by $\delta x_{\mathrm{RMS}} = \sqrt{B\langle P^2\rangle}$. At the resonance frequency, i.e. in FM AFM, the power spectral density reduces to:

$$\langle P^2\rangle = \frac{4k_BT}{C\omega_0^2} \approx Q\frac{4k_BT}{k_L\omega_{0f}} \tag{20}$$

where we used $Q = \omega_{0f} m/C$ as the quality factor of the free cantilever, and assumed $k_{ts} << k_L$ and $\omega_0 \approx \omega_{0f}$ to obtain the approximate result on the right-hand-side.

In sub-resonance AM AFM, the formula (19) instead reduces to:

$$\langle P^2 \rangle = \frac{4k_B TC}{(k_L + k_{ts})^2} \approx \frac{1}{Q} \frac{4k_B T}{k_L \omega_{0f}} \tag{21}$$

Comparing the approximate results (20) and (21), the thermal noise *increases* with increasing quality factor Q if the lever is driven at its resonance (as in FM AFM), and *decreases* in the case of sub-resonance AFM. What does this mean in practice ? In order to reliably measure the frequency or amplitude of a cantilever with a 0.1 Å= 10 pm free amplitude, the rms amplitude of the thermal noise needs to be less than 1 pm. At room temperature, for a lever with a Q of 1000, a resonance frequency of $\omega_{0f} = 2\pi \cdot 200$ kHz, and a measurement bandwidth of 100 Hz, the cantilever stiffness would need to be about 1,300 N/m in the case of FM AFM, and 1.3×10^{-3} N/m in the case of sub-resonance AM AFM. A cantilever of 1,300 N/m would provide a frequency shift of 7.7 Hz for an interaction stiffness of 0.1 N/m. The thermal *frequency* noise can be calculated from [27, 45]:

$$\delta f_{\mathrm{RMS}} = \sqrt{\frac{k_B T B f_{0f}}{k_L A_0^2 \pi Q}} \tag{22}$$

This gives a thermal frequency noise of 14 Hz for a lever of 1,300 N/m. The lever amplitude therefore would need to be somewhat increase beyond this value to get a force gradient sensitivity of 0.1 N/m. A cantilever of such high stiffness may sound difficult to implement, but a lever stiffness of 1,800 N/m has recently been used by Giessibl to achieve unprecedented high resolution on Si 7x7 surfaces [39, 46].

In the case of sub-resonance AM AFM, the lever stiffness would have to be increased far beyond the thermal noise limit of 1.3×10^{-3} N/m to about 100 N/m to avoid snap-to-contact. In this case the rms amplitude of the thermal noise would reduce to 3.6 fm, which is more than sufficient for even the most stringent requirements. At a lever stiffness of 100 N/m, a force gradient of 0.1 N/m would result in a change of the lever amplitude of about 10 fm assuming a free lever amplitude of 0.1 Å= 10 pm , i.e. the signal would be a factor of three above the thermal noise limit. Of course, measuring 10 fm even with an interferometric sensor is not an easy task. Measurements of this order have been demonstrated recently [43, 47, 48]. Theoretically, much higher sensitivity is possible if more elaborate interferometric methods are used (see for example in gravitational wave detection: [49]).

Thermal noise can of course also be reduced by lowering the temperature of the instrument [50]. However, the rms amplitude only scales with the square root of the temperature, and thus the expected reduction in thermal noise is 'only' of the order of about 10. On the other hand, there are many additional advantages of low temperature operation, such as limiting drift and surface diffusion, and low temperature operation can provide a significant advantage over room temperature methods.

A short history of small amplitude AFM

Nanoindentation and force controlled AFM

Nanoindentation [51] is a technique to measure contact-mechanical properties on the nanoscale. It essentially operates by indenting a very sharp diamond tip into a surface while monitoring the displacement and the applied load. In 1987, Pethica and Oliver [15] improved this technique by additionally applying a force modulation. This force modulation was small enough ($\approx 10^{-8}$ N) such that, at the observed contact stiffnesses, sub-Ångstrom tip amplitudes were generated. Such small amplitudes allowed the simultaneous linear measurement of the contact stiffness in addition to the load-displacement curve. From the contact stiffness the size of the contact area could be determined. In their paper the authors also suggested to operate an AFM in a similar fashion, by applying a small AC force to the cantilever via a magnetic transducer.

In 1993, Jarvis et al. demonstrated a force-controlled AFM [52] that used a cantilever with an attached magnet and an electromagnet to apply a DC and small sub-resonance AC force to the cantilever. The small applied AC force resulted in a very small amplitude (≈ 0.3Å) of the cantilever, giving a direct measure of the stiffness of the cantilever-surface system via equation (9). The amplitude was measured with a heterodyne interferometer. The AFM was able to detect a negative stiffness region under ambient condition, which is difficult to achieve with conventional AFM due to the snap-in instability. This device was subsequently implemented in ultra-high vacuum [53], resulting in the first direct measurement of the interaction stiffness between clean surfaces [54]. Imaging with the force controlled AFM was also demonstrated [55]. This technique was also used in liquids, where O'Shea et al. have successfully used the force controlled AFM to measure solvation forces [56, 57] in several organic solvents. They used amplitudes of a few Å which were appropriate for the relatively large molecules they studied.

On-resonance AM AFM

In usual AM or tapping mode AFM, a displacement rather than a force is applied to the cantilever. If the applied displacement is small enough, the at-resonance amplitude of the lever can be kept in the Ångstrom regime, depending on the Q and k_L of the lever (see our discussion of thermal noise above).

Erlandsson et al. demonstrated an on-resonance AM AFM technique [58] with small free amplitudes of < 10 Å. The needed sensitivity was provided by the use of a fiber interferometer [59]. During imaging the amplitude was reduced by 20-90% of the free value due to the shift of the resonance frequency. Using this technique, true atomic resolution on silicon (111)-(7x7) surfaces [60] was achieved. However, due to the use of an on-resonance technique, and the still relatively large amplitudes, the interpretation of the amplitude data proved difficult [61].

FM AFM

In FM AFM, cantilever stiffnesses of 10-50 N/m and large amplitudes of 10 - 50 nm [45] are generally used. The large amplitudes provide good stability and signal-to-noise and are thus preferred when imaging with atomic resolution [29]. There are rather few examples of FM AFM experiments that utilized amplitudes less than 10

nm. Kitamura et al. have used amplitudes as low as 1.5 nm to image Si(111) [62]. Recently, Eguchi et al. used amplitudes of 2.8 nm to also image Si(111) and were able to resolve rest atoms [63]. The main reason for the low number of small amplitude experiments is the use of low stiffness cantilevers, which require large amplitudes to avoid the snap-in instability (see equation (18)).

Stable small amplitude operation at resonance requires very stiff levers in order to avoid the snap-in instability and to reduce thermal noise. Recently, Giessibl designed a novel force sensor based on a quartz tuning fork [39]. This sensor has a very high stiffness of 1,300 - 1,800 N/m. Using this new device he was able to achieve very stable atomic resolution imaging at amplitudes of 4 Å, which is very small for FM AFM.

Using the same setup, Giessibl et al. recently achieved sub-atomic (orbital) resolution of the tip and the Si substrate [46, 64]. Better-than-atomic resolution had previously only been observed in STM measurements. A tuning fork based sensor was found to also provide atomic resolution and atomic scale friction measurements in a small amplitude (3 Å) *lateral* mode [65].

Giessibl at al. have argued that in FM AFM measurements, small amplitudes and large cantilever stiffnesses should be able to *improve* signal-to-noise [45]. This depends on the exact nature and magnitude of any dissipative processes. Despite the presence of energy dissipation, the advantages of small amplitudes and stiff cantilevers in FM AFM have been experimentally confirmed [39,46,64]. A possible reason for the improved S/N of small amplitude techniques is that the tip will spend most of its time in the regime of *short-range* forces when small amplitudes are used close to the surface [66]. These forces are ultimately responsible for atomic resolution imaging. Large amplitude techniques are more affected by long-range forces (e.g. van-der-Waals), thus degrading sensitivity to short-range bonding forces. The same reasoning has recently applied to the room temperature observation of rest atoms in Si(111)-(7x7) at reduced amplitudes of 2.8 nm [63].

Sub-resonance AM AFM

Thermal noise and limits of sensitivity are the most important obstacles in reducing the vibration amplitude of the cantilever into the linear regime of a few 0.1 Å. There are essentially two ways to limit thermal noise: High stiffness cantilevers and sub-resonance operation. Sensitivity can be improved by using new detection schemes, such as tuning forks for FM detection [64] and fiber interferometers for AM detection [59].

Recently, Oral et al. [67] constructed a fiber interferometer based AFM which was optimized to operate at ultra-small amplitudes of < 0.25 Å. This instrument has since been successfully used to obtain atomic-resolution maps of the force gradient on Si(111) [47] and Si(100) [68, 69], to measure atomic bonding forces between a W tip and a clean Si(111) surface [43], and to observe atomic scale energy dissipation at amplitudes as low as 0.13 Å on Cu(100) [48] and with slightly larger amplitudes on Si(100) [68, 69].

Sub-resonance detection can also be used in liquids. Although the thermal noise increases somewhat due to the decrease in Q (see equation (21)), sub-resonance AM detection is better suited for liquid-based measurements, since there is no need to measure the resonance frequency under low Q conditions. Recently, sub-resonance AFM has been used at an amplitude of 0.35 Å for the first *direct* AFM measurement [71] of the molecular stiffness variations of confined

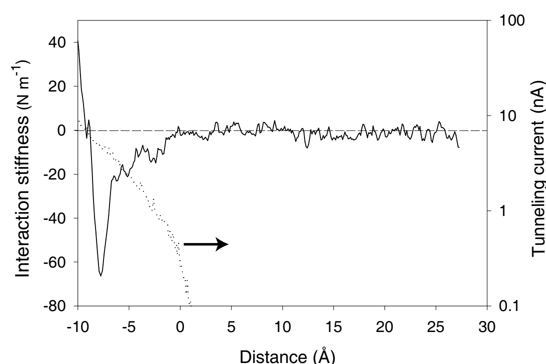

Figure 3: Directly measured stiffness of an atomic bond between a tungsten tip and a clean Si(111) surface in UHV. In addition to the stiffness of the bond, data also includes the longer-range van-der-Waals interaction between the tip and the surface. Long- and short-range forces can be separated by using a suitable fitting procedure [43, 72] Also shown is the simultaneously acquired tunneling current.

water layers [33].

Force gradients of chemical bonds

Few methods allow the direct measurement of the distance-dependent interactions between single atoms. Recently, large amplitude dynamic AFM has been used to achieve this goal [50, 72]. However, there are a few remaining questions, especially the difference of the observed interaction length range measured in low temperature [50] versus room temperature [72] measurements. Part of the problem might be the dissipative interactions which are not always accounted for in the deconvolution schemes used in large amplitude measurements.

Unambiguous measurements of conservative and dissipative interactions can be achieved by low amplitude measurements. Recently, sub-resonance, ultra-small ($\approx$ 0.2 – 0.25 Å) amplitude AFM has been applied to measure atomic interactions between a tungsten tip and a clean Si(111)-(7x7) surface at room temperature [43](see Figure 3). No temperature related broadening of the interaction was observed in contrast to some large amplitude measurements [72]. The measured interaction parameters were in agreement with reported theoretical values [73]. Atomic bonding stiffnesses have also been measured on Cu(100) [48] and Si(100) surfaces [68, 69].

Force gradient atomic resolution imaging

One problem of sub-resonance, ultra-small amplitude AFM is that signals are exceedingly small, while the drive frequency can be quite low. This necessitates long integration times for the lock-in detection of the amplitude or phase, which in turn makes it very difficult to use the lock-in signal for feedback during imaging. Imaging has so far been achieved by using the tunneling current for the feedback, while independently imaging the force gradient signal. Using this approach, atomic resolution images of the force gradient have been achieved on Si(111) (see **Figure 1**) [47], Si(100) [68, 69], and Cu(100) [70]. The force gradient images showed atomic contrast independent of the contrast in the tunneling channel. In the case of Cu(100), atomic contrast was seen in the force gradient image even when no atomic contrast was visible in the tunneling image.

Force gradient feedback is possible by using FM detection [39] or by increasing the drive frequency of the lever. The latter can be achieved by increasing the natural resonance frequency of the lever. A higher resonance frequency al-

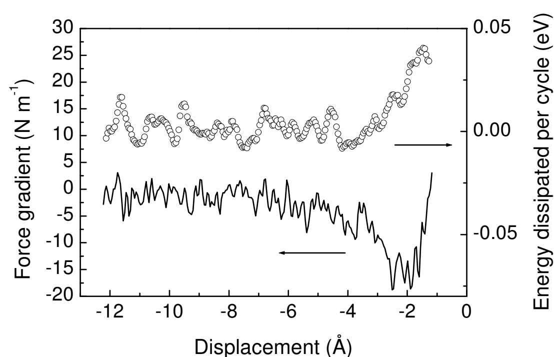

Figure 4: Simultaneously measured interaction stiffness and atomic-scale energy dissipation measured with a tip vibrating at 0.13 Å close to a clean Cu(100) surface in UHV. Note that this measurement was performed close to the noise limit of this particular instrument.

lows for a higher drive frequency, making imaging possible.

Atomic dissipation

A topic of significant interest is the measurement of atomic scale dissipation in AFM. It has been observed in both large [37, 74, 75] and small amplitude [48] UHV-based AFM that the cantilever looses a few meV to eV of kinetic energy per cycle when it is near the surface. A general consensus seems that the observed dissipation is related to 'slow' stochastic motion of atoms at the tip or the sample surface [48, 76].

Small amplitude AFM is expected to be more sensitive to short-range forces [66], and thus to atomic scale dissipation [77]. Small amplitude, sub-resonance AFM is ideally suited to explore dissipation phenomena since any phase difference between drive and lever can be directly related to energy dissipation if the lever is operated in the linear regime far from resonance. Large amplitude techniques can exhibit phase differences merely due to the inherent non-linearities of the system [78, 79]. Recently, sub-resonance, ultra-small amplitude AFM ($A_0 = 0.13$Å) has been used to measure atomic dissipation on a Cu(100) surface [48] (**Figure 4**). It was found that the observed dissipation of a few 10 meV per cycle could be explained by the coupling of the tip motion to the stochastic motion of a surface atom or defect encountering a energy barier of the order of 0.5 eV, i. e. of the order of typical surface diffusion barriers.

Solvation forces - Sub-resonance AFM in liquids

Sub-resonance AFM has the distinct advantage of not relying on a measurement of the resonance frequency, which can be exceedingly difficult if the AFM is operated in a highly damping medium, such as water. Exploiting this fact, it was recently shown that sub-resonance AFM is capable of directly measuring the stiffness oscillations associated with the molecular ordering of water confined between the tip and a flat surface (**Figure 5**). [71]. The advantage of the technique was the unambiguous interpretation of the data and the easy separability of conservative and dissipative terms. This was not possible in earlier large amplitude AFM measurements of the same phenomenon [80].

Conclusions and Outlook

Small amplitude AFM offers distinctive advantages over large amplitude techniques. These include:

1. Linear measurements.

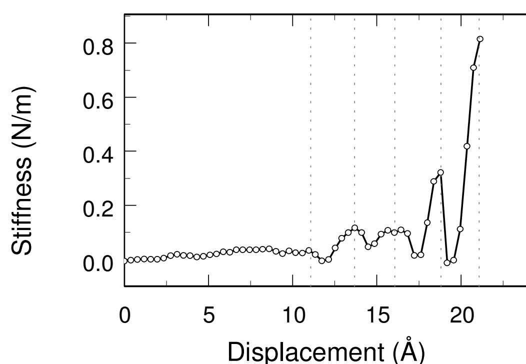

Figure 5: Stiffness of a confined water layer measured with a sub-resonance AFM at a free amplitude of 0.35 Å. Note the regular spacing of higher stiffness separations, corresponding to positions of the tip that allow the confined water to attain a solid-like structure. Intermediate positions are not commensurate with the molecule size of water, and thus result in a low stiffness, disordered layer.

2. Easy data interpretation.
3. Point-by-point, local measurements.
4. Higher sensitivity to short-range forces and potentially better S/N.
5. Easy separation of conservative and dissipative forces, especially when sub-resonance methods are used.
6. Easier transfer to different environments, especially liquids.

The downside of the techniques is the inherently low signals that need to be measured. However, as we have seen, high stiffness cantilevers can reduce thermal noise and high sensitivity displacement sensors are now available which can push amplitude sensitivity into the femtometer regime.

The two most significant developments in this field are the use of sub-resonance techniques and small amplitude FM detection schemes. The sub-resonance techniques offer simple data interpretation, low thermal noise, the possibility of using lower stiffness levers (as long as the snap-in is avoided), and the easy transfer of the technique into liquid environments. The recent experiments using FM detection at small amplitudes are also very encouraging as they combine the advantages of small amplitudes with the high signal-to-noise of FM detection. The very high stiffness levers used in the technique can keep Q values high even in liquids. This opens up the use of FM detection in liquid environments without the need of Q control techniques, which raise additional interpretation issues.

In the future, it is anticipated that small amplitude techniques will play an ever increasing role in *quantitative* AFM measurements. As they operate in virtually *any* environment, the impact on diverse fields, from atomic & molecular manipulation to the nanomechanics of biomolecules could be enormous. If the widely heralded nanotechnology industry is to become a reality, methods that can reliably measure forces, stiffnesses and dissipation at the nanoscale will be essential. Small amplitude AFM might well be the technique of choice to put hard numbers on the workings of the molecular machinery of future nanodevices.

References

[1] Binnig, G.; Rohrer H.; Gerber Ch.; Weibel E. Surface Studies by Scanning Tunneling Microscopy. Phys. Rev. Lett. **1982**, *49* (1), 57-61.

[2] Coombs J. H.; Pethica J. B. Properties of vacuum tunneling currents - anomalous barrier heights. IBM J. Res. Dev. **1986**, *30* (5), 455-459.

[3] Binnig G.; Quate C. F.; Gerber Ch. Atomic force microscope. Phys. Rev. Lett. **1986**, *56* (9), 930-933.

[4] Giessibl F. J. Atomic resolution of the silicon (111)-(7x7) surface by atomic force microscopy. Science **1995**, *267* (5194), 68-71.

[5] Kitamura S.; Iwatsaku M. Observation of 7x7 reconstructed structure on the silicon (111) surface using ultrahigh vacuum noncontact atomic force microscopy. Jpn. J. Appl. Phys. Part 2 **1995**, *34* (1B), L145-L148.

[6] Ueyama H.; Ohta M.; Sugawara Y.; Morita S. Atomically resolved InP(110) surface observed with noncontact ultrahigh vacuum atomic force microscope. Jpn. J. Appl. Phys. Part 2 **1995**, *34* (8B), L1086-L1088.

[7] Dürig U.; Gimzewski J. K.; Pohl D. W. Experimental observation of forces acting during scanning tunneling microscopy. Phys. Rev. Lett. **1986**, *57* (19), 2403-2406.

[8] Martin Y.; Williams C. C.; Wickramasinghe H. K. Atomic force microscope - force mapping and profiling on a sub 100-Åscale. J. Appl. Phys. **1987**, *61* (10), 4723-4729.

[9] Meyer E.; Heinzelmann H.; Grutter P.; Jung T.; Weisskopf T.; Hidber H.R.; Lapka R.; Rudin H.; Güntherodt H. J. Comparative study of lithium-fluoride and graphite by atomic force microscopy (AFM). Journal of Microscopy - Oxford **1988**, *152*, 269-280.

[10] Yamada H.; Fujii T.; Nakayama K. Experimental study of forces between a tunnel tip and the graphite surface. J. Vac. Soc. A **1988**, *6* (2), 293-295.

[11] Cappella B.; Dietler G. Force-distance curves by atomic force microscopy. Surf. Sci. Rep. **1999**, *34*, 1-104.

[12] Burnham N. A.; Colton R. J. Measuring the nanomechanical properties and surface forces of materials using an atomic force microscope. J. Vac. Soc. A **1989**, *7* (4), 2906-2913.

[13] Burnham N. A. Accounting for the stiffness of the probe and sample in scanning probe microscopy. J. Vac. Sci. Technol. B **1994**, *12* (3), 2219-2221.

[14] Ohnesorge F.; Binnig G. True atomic-resolution by atomic force microscopy through repulsive and attractive forces. Science **1993**, *260* (5113), 1451-1456.

[15] Pethica J. B.; Oliver W. C. Tip Surface Interaction in STM and AFM. Physica Scripta **1987**, *T19*, 61-66.

[16] Giessibl, F. J. Atomic Force Microscopy in Ultrahigh Vacuum. Jpn. J. Appl. Phys., Part 1 **1994**, *33* (6B), 3726-3734.

[17] Pethica J. B.; Sutton A. P. On the stability of a tip and flat at very small separations. J. Vac. Sci. Technol. A **1988**, *6* (4), 2490-2494.

[18] García R.; Pérez R. Dynamic atomic force microscopy methods. Surf. Sci. Rep. **2002**, *47*, 197-301.

[19] Zhong Q.; Inniss D.; Kjoller K.; Elings V. B. Fractured polymer/ silica fiber surface studied by tapping mode atomic force microscopy. Surf. Sci. Lett. **1993**, *290*, L688-L692.

[20] Gleyzes P.; Kuo P. K.; Boccara A. C. Bistable behavior of a vibrating tip near a solid surface. Appl. Phys. Lett. **1990**, *59* (25), 2989-2991.

[21] Tsukada M.; Sasaki N.; Yamura R.; Sato N.; Abe K. Features of cantilever motion in dynamic-mode AFM. Surf. Sci. **1998**, *401* (3), 355-363.

[22] Anczykowski B.; Krüger D.; Fuchs H. Cantilever dynamics in quasinoncontact force microscopy: Spectroscopic aspects. Phys. Rev. B **1996**, *53* (23), 15485-15488.

[23] García R.; A. San Paulo. Dynamics of a vibrating tip near or in intermittent contact with a surface. Phys. Rev. B **2000**, *61* (20), R13381-R13385.

[24] Chen X.; Davies M. C.; Roberts C. J.; Tendler S. J. B.; Williams P. M.; Burnham N. A. Optimizing phase imaging via dynamic force curves. Surf. Sci. **2000**, *460*, 292-300.

[25] Dürig U. Interaction sensing in dynamic force microscopy. New J. Phys. **2000**, *2*, 5.1-5.12.

[26] Stark M.; Stark R. W.; Heckl W. M.; Guckenberger R. Inverting dynamic force microscopy: From signals to time-resolved interaction forces. Proc. Nat. Acad. Sci. **2002**, *99* (13), 8473-8478.

[27] Albrecht T. R.; Grütter P.; Horne D.; Rugar D. Frequency modulation detection using high-Q can-

tilevers for enhanced force microscopy sensitivity. J. Appl. Phys. **1991**, *69* (2), 668-673.

[28] Giessibl F. J. Forces and Frequency shifts in atomic-resolution dynamic-force microscopy. Phys. Rev. B **1997**, *56* (24), 16010-16015.

[29] Schwarz U. D.; Hölscher H.; Wiesendanger R. Atomic resolution in scanning force microscopy: Concepts, requirements, contrast mechanisms, and image interpretation. Phys. Rev. B **2000**, *62* (19), 13089-13097.

[30] Ke S. H.; Uda T.; Terakura K. Quantity measured in frequency-shift-mode atomic-force miscroscopy: An analysis with a numerical model. Phys. Rev. B **1999**, *59* (20), 13267-13272.

[31] Giessibl F. J. A direct method to calculate tip-sample interaction forces from frequency shifts in frequency-modulation atomic force microscopy. Appl. Phys. Lett. **2001**, *78* (1), 123-125.

[32] Tamayo J.; Humphris A. D. L.; Miles M. J. Piconewton regime dynamic force microscopy in liquids. Appl. Phys. Lett. **2000**, *77* (4), 582-584.

[33] Israelachvili J. *Intermolecular & Surface Forces*; Academic Press: London, 1992.

[34] Hoffmann P. M. Dynamics of small amplitude, off-resonance AFM. Appl. Surf. Sci. **2003**, *210*, 140-145.

[35] Rabe U.; Janser K.; Arnold W. Vibrations of free and surface-coupled atomic force microscope cantilevers: Theory and experiment. Rev. Sci. Instr. **1996**, em 67 (9), 3281-3293.

[36] Hölscher H.; Schwarz U. D.; Wiesendanger R. Calculation of the frequency shift in dynamic force microscopy. Appl. Surf. Sci. **1999**, *140*, 344-351.

[37] Gotsmann B.; Seidel C.; Anczykowski B.; Fuchs H. Conservative and dissipative tip-sample interaction forces probed with dynamic AFM. Phys. Rev. B **1999**, *60* (15), 11051-11060.

[38] Chen G. Y.; Warmack R. J.; Huang A.; Thundat T. Harmonic response of near-contact scanning force microscopy. J. Appl. Phys. **1995**, *78* (3), 1465-1469.

[39] Giessibl F. J. Atomic resolution on Si(111)-(7x7) by noncontact atomic force microscopy with a force sensor based on a quartz tuning fork. Appl. Phys. Lett. **2000**, *76* (11), 1470-1472.

[40] Sarid D.; Elings V. Review of Scanning Force Microscopy. J. Vac. Sci. Technol. B **1991**, *9* (2), 431-437.

[41] Sarid D. *Scanning Force Microscopy*; Oxford Univ. Press: Oxford, 1994.

[42] Gustafsson M. G. L.; Clarke J. Scanning force microscope springs optimized for optical-beam deflection and with tips made by controlled fracture. J. Appl. Phys. **1994**, *76*, 172-181.

[43] Hoffmann P. M.; Oral A.; Grimble R. A.; Özer H. Ö.; Jeffery S.; Pethica J. B. Direct measurement of interatomic force gradients using an ultra-low-amplitude atomic force microscope. Proc. R. Soc. Lond. A **2001**, *457*, 1161-1174.

[44] Saulson P. R. Thermal noise in mechanical experiments. Phys. Rev. D **1990**, *42* (8), 2437-2445.

[45] Giessibl F. J.; Bielefeldt H.; Hembacher S.; Mannhart J. Calculation of the optimal imaging parameters for frequency modulation atomic force microscopy. Appl. Surf. Sci. **1999**, *140*, 352-257.

[46] Giessibl F. J.; Bielefeldt H.; Hembacher S.; Mannhart J. Imaging of atomic orbitals with the Atomic Force Microscope - experiments and simulations. Ann. Phys. **2001**, *10* (11-12), 887-910.

[47] Oral A.; Grimble R. A.; Özer H. Ö.; Hoffmann P. M.; Pethica J. B. Quantitative atom-resolved force gradient imaging using noncontact atomic force microscopy. Appl. Phys. Lett. **2001**, *79* (12), 1915-1917.

[48] Hoffmann P. M.; Jeffery S.; Pethica J. B.;Özer H. Ö.; Oral A. Energy dissipation in atomic force microscopy and atomic loss processes. Phys. Rev. Lett. **2001**, *87* (26), 265502 (1-4).

[49] Ju L.; Blair D. G.; Zhao C. Detection of gravitational waves Rep. Prog. Phys. **2000**, *63* (9), 1317-1427.

[50] Lantz M. A.; Hug H. J.; van Schendel P. J. A.; Hoffmann R.; Martin S.; Baratoff A.; Abdurixit A.; Güntherodt H.-J.; Gerber Ch. Low temperature scanning force microscopy of the Si(111)-(7x7) surface. Phys. Rev. Lett. **2000**, *84* (12), 2642-2645.

[51] Pethica J. B.; Hutchings R.; Oliver W. C. Hardness measurement at penetration depths as small as 20 nm. Phil. Mag. A **1983**, *48* (4), 593-606.

[52] Jarvis S. P.; Oral A.; Weihs T. P.; Pethica J. B. A novel force microscope and point contact probe. Rev. Sci. Instr. **1993**, *64* (12), 3515-3520.

[53] Jarvis S. P.; Yamada H.; Yamamoto S.-I.; Tokumoto H. A new force controlled atomic force microscope for use in ultrahigh vacuum. Rev. Sci. Instrum. **1996**, *67* (6), 2281-2285.

[54] Jarvis S. P.; Yamada H.; Yamamoto S.-I.; Tokumoto H.; Pethica J. B. Direct mechanical measurement of interatomic potentials. Nature **1996**, *384*, 247-249.

[55] Jarvis S. P.; Lantz M. A.; Dürig U.; Tokumoto H. Off resonance ac mode force spectroscopy and imaging with an atomic force microscope. Appl. Surf. Sci. **1999**, *140*, 309-313.

[56] O'Shea S. J.; Welland M. E.; Pethica J. B. Atomic force microscopy of local compliance at solid-liquid interfaces. Chem. Phys. Lett. **1994**, *223*, 336-340.

[57] O'Shea S. J.; Welland M. E. Atomic force microscopy at solid-liquid intefaces. Langmuir **1998**, *14*, 4186-4197.

[58] Olsson L.; Wigren R.; Erlandsson R. Ultrahigh vacuum scanning force/ scanning tunneling microscope: Application to high resolution imaging of Si(111)7x7. Rev. Sci. Instr. **1996**, *67* (6), 2289-2296.

[59] Rugar D.; Mamin H. J.; Erlandsson R.; Stern J. E.; Terris B. D. Force microscope using a fiber-optic displacement sensor. Rev. Sci. Instr. **1988**, *59* (11), 2337-2340.

[60] Erlandsson R.; Olsson L.; Mårtensson P. Inequivalent atoms and imaging mechanisms in ac-mode atomic-force microscopy of Si(111)7x7. Phys. Rev. B **1996**, *54* (12), R8309-R8312.

[61] Erlandsson R.; Olsson L. Force interaction in low-amplitude ac-mode atomic force microscopy: cantilever simulations and comparison with data from Si(111)7x7. Appl. Phys. A **1998**, *66*, S879-883.

[62] Kitamura S.; Iwatsuki M. Observation of silicon surfaces using ultrahigh-vacuum noncontact atomic force microscopy. Jpn. J. Appl. Phys. Part 2 **1996**, *35* (5B), L668-L671.

[63] Eguchi T.; Hasegawa Y. High resolution atomic force microscopic imaging of the Si(111)-(7x7) surface: contribution of short-range forces to the images. Phys. Rev. Lett. **2002**, *89* (26), 266105 (1-4).

[64] Giessibl F. J.; Hembacher S.; Bielefeldt H.; Mannhart J. Subatomic features on the Si(111)-(7x7) surface observed by atomic force microscopy. Science **2000**, *289* (5478), 422-425.

[65] Giessibl F. J.; Herz M.; Mannhart J. Friction traced to the single atom. Proc. Nat. Acad. Sci. **2002**, *99* (19), 12006-12010.

[66] Giessibl F. J.; Bielefeldt H. Physical interpretation of frequency-modulation atomic force microscopy. Phys. Rev. B **2000**, *61* (15), 9968-9971.

[67] Oral A.; Grimble R. A.; Özer H. Ö.; Pethica J. B. High-sensitivity noncontact atomic force microscope/scanning tunneling microscope (nc AFM/STM) operating at subangstrom oscillation amplitudes for atomic resolution imaging and force spectroscopy. Rev. Sci. Instr. **2003**, *74* (8), 3656-3662.

[68] Özer H. Ö.; Mehrdad A.; Oral A. Ultra-small oscillation amplitude nc-AFM/STM imaging, force and dissipation spectroscopy of Si(100)(2 x 1). Solid State Communications **2002**, *124* (12), 469-472.

[69] Özer H. Ö.; Mehrdad A.; Oral A. Measurement of energy dissipation between tungsten tip and Si(100)-(2x1) using sub-Ångström oscillation amplitude non-contact atomic force microscope. Appl. Surf. Sci. **2003**, *210*, 12-17.

[70] Özer H. Ö.;Norris A.; Oral A.; Hoffmann P. M.; Pethica J. B. Low amplitude, force gradient imaging of Cu(100) surface using tunnel current feedback. Nanotechnology **2004**, *15*, S5-S8.

[71] Hoffmann P. M.; Jeffery S.; Oral A.; Grimble R. A.; Özer H. Ö.; Pethica J. B. Nanomechanics using an ultra-small amplitude AFM. Mat. Res. Soc. Symp. Proc. **2001**, *649*, Q9.2.1-6.

[72] Guggisberg M.; Bammerlin M.; Loppacher C.; Pfeiffer O.; Abdurixit A.; Barwich V.; Bennewitz R.; Baratoff A.; Meyer E.; Guntherodt H. J. Separation of interactions by noncontact force microscopy. Phys. Rev. B **2000**, *61* (16), 11151-11155.

[73] Pérez R.; Štich I.; Payne M. C.; Terakura K. Surface-tip interactions in noncontact atomic-force microscopy on reactive surfaces: Si(111). Phys. Rev. B **1998**, *58* (16), 10835-10849.

[74] Loppacher C.; Bennewitz R.; Pfeiffer O.; Guggisberg M.; Bammerlin M.; Schär S.; Barwich V.; Baratoff A.; Meyer E. Experimental aspects of dissipation force microscopy. Phys. Rev. B **2000**, *62* (20), 13674-13679.

[75] Gotsmann B.; Fuchs H. Dynamic force spectroscopy of conservative and dissipative forces in an Al-Au(111) tip-sample system. Phys. Rev. Lett. **2001**, *86* (12), 2597-2600.

[76] Sasaki N.; Tsukada M. Effect of microscopic nonconservative process on noncontact atomic force microscopy. Jpn. J. Appl. Phys. Part 2 **2000**, *39*(12B), L1334-L1337.

[77] Gauthier M.; Tsukada M. A theoretical study on mass sensitive surface analysis and subsurface imag-

ing with dynamic force microscopy. Surf. Sci. **2001**, *495* (3), 204-210.

[78] Gauthier M.; Tsukada M. Damping mechanism in dynamic force microscopy. Phys. Rev. Lett. **2000**, *85* (25), 5348-5351.

[79] Gauthier M.; Pérez R.; Arai T.; Tomitori M.; Tsukada M. Interplay between nonlinearity, scan speed, damping, andelectronics in frequency modulation atomic-force microscopy. Phys. Rev. Lett. **2002**, *89* (14), 146104.

[80] Jarvis S. P.; Uchihashi T.; Ishida T.; Tokumoto H.; Nakayama Y. Local solvation shell measurement in water using a carbon nanotube probe. J. Phys. Chem B **2000**, *104* (26), 6091-6094.